JPn Neuroscience

The Journal of Physiology

J Physiol 591.13 (2013) pp 3325–3340

A 'toothache tree' alkylamide inhibits Aδ mechanonociceptors to alleviate mechanical pain

Makoto Tsunozaki[1,*], Richard C. Lennertz[2,*], Daniel Vilceanu[2], Samata Katta[1], Cheryl L. Stucky[2] and Diana M. Bautista[1,3]

[1] *Department of Molecular and Cell Biology, UC Berkeley, Berkeley, CA 94720, USA*
[2] *Department of Cell Biology, Neurobiology and Anatomy, Medical College of Wisconsin, Milwaukee, WI 53226, USA*
[3] *Helen Wills Neuroscience Institute, UC Berkeley, Berkeley, CA 94720, USA*

Key points

- Extracts from the toothache tree (*Zanthoxylum*) are used to treat inflammatory pain, such as toothache and arthritis.
- Hydroxy-α-sanshool (sanshool) is a major alkylamide in extracts from *Zanthoxylum* plants.
- Sanshool treatment in mice caused a selective attenuation of mechanical sensitivity under naïve and inflammatory conditions
- Sanshool inhibits Aδ mechanonociceptors that mediate both sharp acute pain and inflammatory pain, and inhibits the activity of multiple voltage-gated sodium channel subtypes, among which $Na_v1.7$ is the most strongly affected.
- Our data implicate $Na_v1.7$ as a key mediator of inflammatory mechanical pain in 'fast pain' mechanosensory neurons.

Abstract In traditional medicine, the 'toothache tree' and other plants of the *Zanthoxylum* genus have been used to treat inflammatory pain conditions, such as toothache and rheumatoid arthritis. Here we examined the cellular and molecular mechanisms underlying the analgesic properties of hydroxy-α-sanshool, the active alkylamide produced by *Zanthoxylum* plants. Consistent with its analgesic effects in humans, sanshool treatment in mice caused a selective attenuation of mechanical sensitivity under naïve and inflammatory conditions, with no effect on thermal sensitivity. To elucidate the molecular mechanisms by which sanshool attenuates mechanical pain, we performed single fibre recordings, calcium imaging and whole-cell electrophysiology of cultured sensory neurons. We found that: (1) sanshool potently inhibits Aδ mechanonociceptors that mediate both sharp acute pain and inflammatory pain; (2) sanshool inhibits action potential firing by blocking voltage-gated sodium currents in a subset of somatosensory neurons, which express a unique combination of voltage-gated sodium channels; and (3) heterologously expressed $Na_v1.7$ is most strongly inhibited by sanshool as compared to other sodium channels expressed in sensory neurons. These results suggest that sanshool targets voltage-gated sodium channels on Aδ mechanosensory nociceptors to dampen excitability and thus induce 'fast pain' analgesia.

(Resubmitted 23 January 2013; accepted after revision 3 May 2013; first published online 7 May 2013)

Corresponding author D. M. Bautista: Life Science Addition room 355, Berkeley, CA 94720-3200, USA. Email: dbautista@berkeley.edu; C. L. Stucky: 8701 Watertown Plank Road, Milwaukee, WI 53226, USA. Email: cstucky@mcw.edu

Abbreviations AM fibre; Aδ mechanoreceptor fibre; AP, action potential; D hair, down hair; DMF, dimethylformamide; DRG, dorsal root ganglion; LA, local anaesthetic; Na_v channel, voltage-gated sodium channel; qPCR, quantitative PCR; sanshool, hydroxy-α-sanshool

M. Tsunozaki and R. C. Lennertz contributed equally to this work.

DOI: 10.1113/jphysiol.2013.252106x

Introduction

Zanthoxylum plants (such as prickly ash) are also known as 'toothache trees' due to the analgesic properties of their bark and fruit. Native cultures from around the world, including Native American, African, South Asian and Chinese traditions have used prickly ash and related plants to treat toothache, arthritis and pain through topical application for hundreds of years (Foster & Duke, 1999; Pereira *et al.* 2010). The two most common sites of treatment by prickly ash, the teeth and joints, are richly innervated by pain fibres, suggesting that active chemicals within prickly ash may directly target peripheral pain neurons.

Distinct somatosensory neuron subtypes mediate sensitivity to touch and pain. They are classified as Aβ, Aδ and C fibres based on unique morphologies, mechanical response thresholds and electrophysiological properties (Iggo, 1960; Brown & Iggo, 1967; Harper & Lawson, 1985; Smith & Lewin, 2009; McGlone & Reilly, 2010; Lumpkin *et al.* 2010). Aβ fibres are heavily myelinated, have larger cell bodies, have terminals that interact with accessory cells in the skin, and function as innocuous touch receptors. Aβ fibres that exhibit a transient, phasic response to a constant stimulus are classified as 'rapidly adapting', whereas those that have a tonic response are called 'slowly adapting'. C fibres are unmyelinated, have smaller cell bodies, terminate as free nerve endings in the skin, and many detect harmful mechanical, thermal and chemical stimuli. Aδ fibres are lightly myelinated and tend to have intermediate cell body sizes. Most slowly adapting Aδ fibres (AM fibres) are mechanoreceptors activated by intense (presumably noxious) mechanical stimuli, while rapidly adapting Aδ fibres (D hairs) detect innocuous tactile stimuli to hairy skin.

Underlying the morphological and physiological diversity of somatosensory neurons is a wide diversity of molecular components. In particular, recent studies have shown that somatosensory neurons express a wide array of voltage-gated sodium (Na_v) channel subtypes that dictate excitability (Rush *et al.* 2007). Some Na_v channel subtypes (such as $Na_v1.1$, $Na_v1.2$, $Na_v1.3$ and $Na_v1.6$) are expressed in both the central and peripheral nervous systems. In contrast, three Na_v subtypes ($Na_v1.7$, $Na_v1.8$ and $Na_v1.9$) are predominantly expressed in the somatosensory system, where these channels are thought to play critical functional roles (Rush *et al.* 2007). For example, C fibre nociceptors are enriched in $Na_v1.8$ and $Na_v1.9$, two Na_v subtypes that are unique in their resistance to the potent sodium channel blocker tetrodotoxin (TTX). $Na_v1.8$ plays a role in maintaining action potential (AP) transmission under cold, and contributes to lidocaine resistance in C fibres (Zimmermann *et al.* 2007; Kistner *et al.* 2010). Thus there is much interest in identifying subtype-specific sodium channel blockers that will attenuate excitability in specific subsets of somatosensory fibres and promote analgesia (Eijkelkamp *et al.* 2012).

Here we ask whether the toothache tree promotes analgesia by targeting distinct populations of somatosensory neurons. A relatively abundant component among several alkylamides found in prickly ash (*Zanthoxylum piperitum*) extracts is hydroxy-α-sanshool (sanshool), which induces tingling paraesthesia and numbing analgesia (Bryant & Mezine, 1999; Sugai *et al.* 2005*a*,*b*). Recent studies have shown that sanshool may cause tingling sensations by blocking two-pore potassium channels (Bautista *et al.* 2008) and inducing AP firing in a subset of rapidly adapting myelinated fibres that mediate light touch (Lennertz *et al.* 2010). However, the mechanism by which sanshool induces numbing analgesia is not understood. Here we used behavioural assays, cutaneous sensory fibre recordings, whole-cell patch clamp and calcium imaging to show that sanshool inhibits the excitability of Aδ nociceptive mechanosensory neurons that mediate fast pain by blocking voltage-gated sodium channels.

Methods

Animals

All behavioural protocols were approved by the UC Berkeley Institutional Animal Care and Use Committee, by the Institutional Animal Care and Use Committee at the Medical College of Wisconsin, and were performed in accordance with the guidelines put forth by the National Institutes of Health. Male C57/B6 mice between 8 and 14 weeks old were used. Mice were housed with unrestricted access to food and water and maintained on a 12:12 h light–dark cycle in a controlled environment. Animals were housed individually for all behavioural assays.

Behavioural assays

von Frey, radiant heat and hot plate assays were carried out essentially as described (Hargreaves *et al.* 1988; Chaplan *et al.* 1994; Cao *et al.* 1998). Briefly, animals were acclimated in the corresponding assay chambers starting 2 days before the day of the assay. To induce neurogenic inflammation, 5 μL of 10% allyl isothiocyanate (Sigma, St. Louis, MO, USA) in mineral oil was applied topically to the plantar and hairy surfaces of one hindpaw. For topical application to skin, sanshool was diluted in dimethylformamide (DMF) at 50 mM and 5 μl was applied to the plantar surface of the hindpaw. Sensory thresholds and latencies were tested 30–60 min after application of allyl isothiocyanate or sanshool. All behavioural assays were performed with the experimenter blind to treatment.

Animals were killed by CO_2 inhalation followed by cervical dislocation immediately after all experiments.

Teased nerve fibre recordings

Mice were briefly anaesthetized with isoflurane and killed via cervical dislocation. Subsequently, the skin from the hindpaw along with the saphenous nerve was dissected, placed corium side up and superfused with synthetic interstitial fluid as previously described (Reeh, 1986). The nerve was teased into thin filaments until extracellular recordings were obtained from isolated receptive fields. Data were collected using a PowerLab 4/sp, and were recorded and analysed using the Chart program (v5.5.6; ADInstruments, Colorado Springs, CO, USA). Receptive fields were identified with a mechanical probe. Fibres were characterized according to their conduction velocity, von Frey thresholds and adaptation to a suprathreshold mechanical stimulus as previously described ($A\beta \geq 10\ ms^{-1} > A\delta \geq 1.2\ ms^{-1} > C$) (Koltzenburg *et al.* 1997). Aβ fibres were characterized as slowly adapting if they responded throughout a sustained mechanical force or rapidly adapting if they respond predominantly at the onset or offset of force. Aδ fibres were classified as either slowly adapting AM or rapidly adapting Down hair (D hair) receptors. D hair receptors responded to very low mechanical forces ($\ll$1 mN), whereas AM fibres exhibited mechanical thresholds $\geq$4 mN. Furthermore, D hair receptors had very large receptive fields (up to 8 mm in diameter) whereas AM fibres had very small ($\leq$1 mm) discrete, sensitive receptive field spots. C fibres were all slowly adapting. The minimum AP amplitude for all fibre types was at least threefold greater than the noise level.

Fibres were exposed to sanshool or vehicle (0.2% DMF in synthetic interstitial fluid) for 5 min and stimulated with a 10 mN force for 10 s delivered by a feedback-controlled, computer driven mechanical probe, 0.8 mm in diameter with a smooth flat end (Kwan *et al.* 2009). Fibres were stimulated before exposure to sanshool or vehicle, at 1 min intervals during the exposure to compounds and then at 2 min intervals after the exposure. The same protocol was used for electrical stimulation, except a 10% suprathreshold stimulus was delivered to the receptive field. For concentration and mechanical stimulus dose–responses, AM fibres were exposed to different concentrations of sanshool for 2 min (20, 60, 100 or 200 μM sanshool). Subsequently, these fibres were stimulated with increasing mechanical forces (10, 40, 100 and 200 mN) at 1 min intervals in the presence of sanshool.

Cell and neuron cultures

Chinese hamster ovary cells stably expressing recombinant human $Na_v1.1$, 1.2, 1.3, 1.6, 1.7 or 1.8 (Chantest, Cleveland, OH, USA) were cultured in Ham's F12 media (Life Technologies, Carlsbad, CA, USA) supplemented with 10% foetal bovine serum; $Na_v1.9$-expressing cells were not available. Pilot studies were conducted on human embryonic kidney cells stably expressing recombinant human $Na_v1.7$ (gift from T. Cummins). Dorsal root ganglion (DRG) neuron cultures were prepared as previously described (Bautista *et al.* 2008). Neurons were dissociated from dissected DRGs from adult (>8-week-old) animals. Culture media was minimal essential medium (Life Technologies) supplemented with glutamine (Thermo Scientific, Logan, UT, USA), MEM vitamin (Thermo Scientific) and penicillin-streptomycin (Thermo Scientific). Neurons were plated on round coverslips coated with poly-D-lysine and laminin, as previously described (Malin *et al.* 2007), were incubated overnight at 37°C/5% CO_2, and assayed the following day.

Calcium imaging

Calcium imaging was carried out essentially as described (Lennertz *et al.* 2010). Assays were performed in extracellular Ringer's solution containing (in mM): 140 NaCl, 5 KCl, 10 Hepes, 10 glucose, 2 $MgCl_2$, 2 $CaCl_2$; pH 7.4. An increase in Fura-2 ratio of >20% over baseline was considered a response.

Quantitation of sodium channel mRNA expression

Between three and 10 cultured neurons classified based on their calcium response to sanshool and cell size were collected and pooled in lysis buffer using a pulled glass pipette. Lysis buffer contained (in mM): 75 KCl, 50 Tris-Cl (pH 8.3), 3 $MgCl_2$ with 2 U μL^{-1} RNAsin (Promega, Madison, WI, USA). For a single biological replicate, cells from two to four experiments were pooled and treated with DNase (TURBO DNAfree, Life Technologies). First strand synthesis was carried out according to manufacturer's specifications (Superscript III, Life Technologies). Quantitative PCR (qPCR) was carried out on a StepOnePlus Real-time PCR System using SYBR GreenER reagents (Life Technologies) with primers for Na_v channels described previously (Lopez-Santiago *et al.* 2006). qPCR for each channel subtype was carried out in triplicates. Expression of a channel subtype was defined as amplification of product and determination of a Ct value in two of three replicates within each sample. For quantitation of expression levels, all experiments were normalized to beta actin (forward: cacccgcgagcacagcttctttg, reverse: catgccggagccgttgtcgacg).

Electrophysiology

Whole-cell patch clamp recordings were made with an Axopatch 200B amplifier (Molecular Devices,

Downingtown, PA, USA). Data were sampled at 10 kHz and filtered at 2 kHz. Data were acquired with PClamp10 (Molecular Devices, Natick, MA, USA) and analysed with custom scripts in MATLAB (Mathworks). Fire-polished electrodes (1–2 MΩ) were fabricated from borosilicate glass (Sutter, Instrument Company, Novato, CA, USA). Series resistance was compensated for by 90–95% and capacitance artefact was cancelled using the amplifier circuitry. For current clamp recordings, neurons that had resting membrane potential less than −50 mV were used.

Internal solution for voltage clamp recordings contained (in mM): 140 CsF, 10 NaCl, 5 Hepes, 1 EGTA, 2 $MgCl_2$, 1 MgATP, 0.1 NaGTP 0.1 cAMP; pH 7.3. Internal solution for current clamp recordings contained (in mM): 140 potassium aspartate, 13.5 NaCl, 9 Hepes, 0.09 EGTA, 1.6 $MgCl_2$, 1 MgATP, 0.1 NaGTP; pH 7.3. Standard Ringer's solution was used for current clamp recordings and Chinese hamster ovary cell voltage clamp recordings. For sodium current recordings in DRG neurons, extracellular solutions with reduced sodium contained: (in mM): 70/35/10 NaCl, 50/85/105 choline chloride, 20 TEACl, 5 KCl, 10 Hepes, 10 glucose, 2 $MgCl_2$, 2 $CaCl_2$, 0.1 $CdCl_2$; pH 7.4. All solutions were adjusted to 305–320 mosmol kg^{-1} with 1 M mannitol.

A hydroxypropyl-β-cyclodextrin solution was added at 200 μM to extracellular solutions before addition of either DMF vehicle or sanshool stock. Solutions were subsequently sonicated in a water bath for 3–5 min. TTX was used at a final concentration of 300 nM.

Other reagents

Hydroxy-α-sanshool was purified from ethereal extracts of ground Szechuan peppercorns by Irvine Chemistry Laboratory (Anaheim, CA, USA) or prepared in-house. The purity of the compound was confirmed by H_1-NMR as previously described (Bautista *et al.* 2008). Stock solution of sanshool was dissolved in DMF at 100 mM.

Data analysis

Fura-2 ratios were calculated using Metafluor (Molecular Devices). Cellular electrophysiology data was analysed in Clampfit 10.2 (Molecular Devices). Further analyses and statistical comparisons were carried out in MATLAB (Mathworks). For conductance–potential curves, whole-cell current (I) data were first converted to conductances (G) using the equation $G = I/(V - V_{rev})$, where V is the command potential and V_{rev} is the reversal potential. Subsequently, conductance was fit to the Boltzmann equation $G = G_{max}/(1 + \exp((V_{1/2} - V)/k))$, where G_{max} is the maximum conductance, $V_{1/2}$ is the half-maximal conductance potential and k is a slope factor. For steady-state inactivation curves, normalized current (I_{norm}) was fit to the equation $I_{norm} = 1/(1 + \exp((V - V_h)/k))$, where V_h is the potential for half-maximal reduction in current and k is a slope factor. The double Boltzmann equation, used to fit steady-state inactivation data in DRG neurons, was $I_{norm} = f/(1 + \exp((V - V_{h1})/k_1)) + (1 - f)/(1 + \exp((V - V_{h2})/k_2))$, where f is the fraction of current contributed by one of two classes of Na_v channels with either a higher or lower half-maximal potential for reduction in steady-state current. The value of f was chosen to numerically minimize the confidence intervals of both V_{h1} and V_{h2}. All voltages were adjusted during data analysis according to experimentally measured junction potentials for each corresponding pair of solutions.

Results

Behavioural responses to mechanical stimuli are reduced by sanshool

To examine the analgesic properties of sanshool, we measured the effect of topical application of sanshool on mouse somatosensory behaviours. Topical application of sanshool to the hindpaw plantar surface did not evoke any spontaneous licking, flinching or other obvious behaviours. However, topical sanshool significantly elevated the mechanical thresholds for paw withdrawal, as measured using the von Frey assay 60 min after sanshool application (Fig. 1*A*). In contrast, sanshool did not alter responsiveness to noxious thermal stimuli in the radiant heat paw withdrawal assay (Fig. 1*B*), or the hot plate test (Fig. 1*C*). These results suggest that sanshool specifically reduces baseline sensitivity to mechanical stimuli.

Because sanshool is used as a traditional medicine to treat inflammatory pain, we next measured the effect of sanshool on mechanical and heat sensitivity in a model of neurogenic inflammation. Topical application of mustard oil (10%) induced mechanical and heat hypersensitivity that was observed as a significant reduction in mechanical threshold for paw withdrawal and thermal paw withdrawal latency (Fig. 1*D*). Following induction of hypersensitivity by mustard oil, topical application of sanshool greatly attenuated the decrease in mechanical threshold while vehicle had no effect (Fig. 1*D*). Similar to its effect on naïve animals, sanshool did not alter hypersensitivity to noxious heat stimuli during mustard oil-induced neurogenic inflammation (Fig. 1*E*). Thus, sanshool selectively attenuates mechanical pain hypersensitivity.

Sanshool suppresses the mechanosensitivity of somatosensory fibres

We next used the *ex-vivo* skin–nerve preparation to determine if sanshool alters sensory transduction in the

peripheral nervous system, and if so, whether sanshool targets specific subsets of somatosensory fibre types. As we have shown previously that sanshool activates rapidly adapting Aβ and Aδ fibres as well as a subset of C fibre nociceptors (Lennertz *et al.* 2010), we focused our study on fibres that display little or no sanshool-evoked excitation (Table 1). Nerve fibres were mechanically stimulated while the receptive fields were exposed to either vehicle

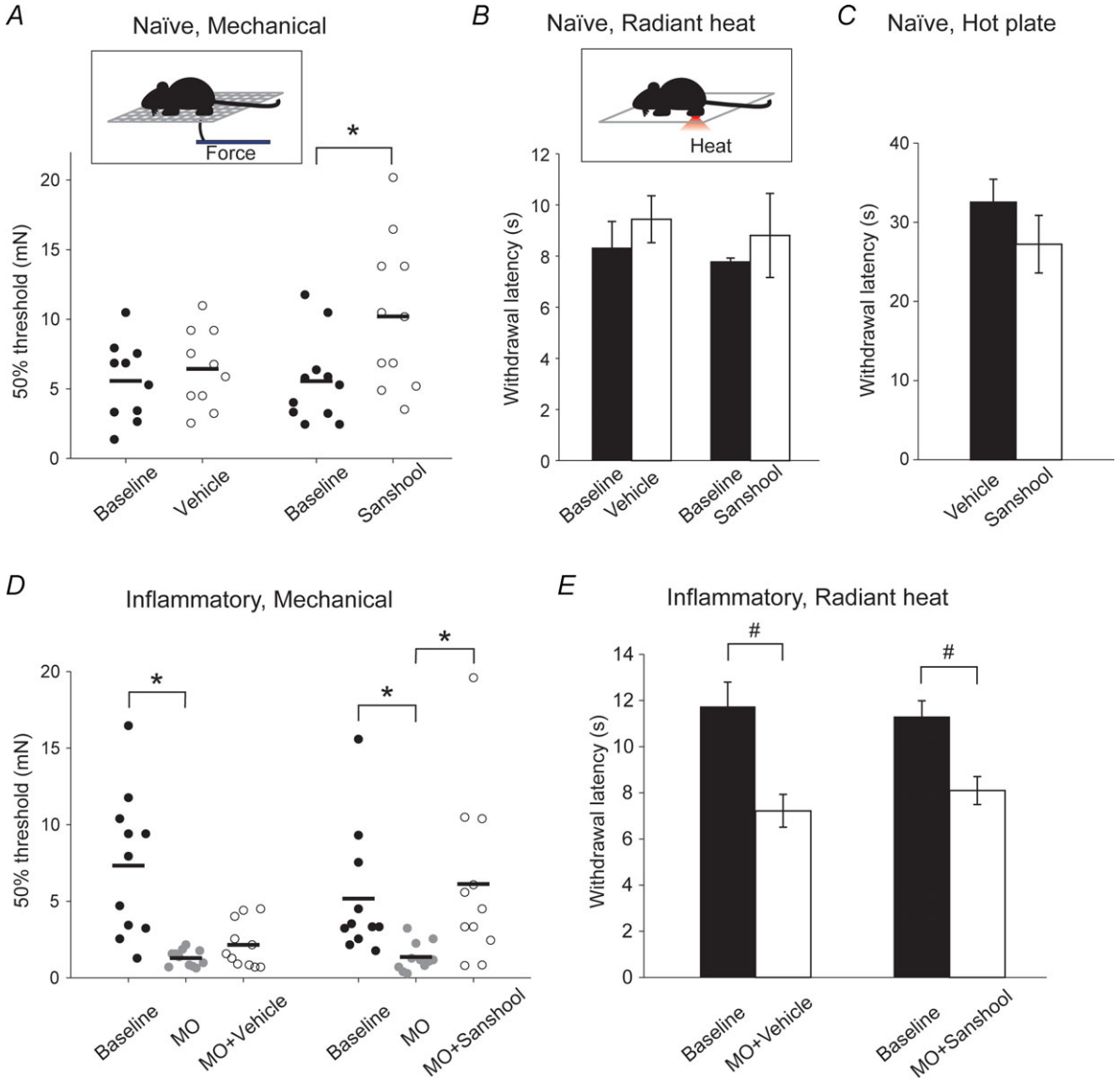

Figure 1. Sanshool increases behavioural response thresholds for mechanical, but not thermal, stimuli
A, individual von Frey response thresholds for naïve animals before and 60 min after topical treatment with vehicle or sanshool on the plantar surface of the hindpaw. Solid bar represents the mean threshold. $n = 10$. $^*P < 0.05$ (Mann–Whitney *U* test). *B*, response latency to radiant heat stimuli applied to the hindpaw, before and after topical treatment with vehicle or sanshool. $n = 6$. *C*, response latency after being placed on a hot plate at 48°C. Either vehicle solution or sanshool was topically applied to the plantar surface of both hindpaws 50 min before placing the animal on the hot plate. $n = 13$ and 9 for vehicle and sanshool, respectively. *D*, von Frey response thresholds for individual animals before and after topical application of mustard oil (MO). After the baseline measurement, MO was applied topically to the hindpaw, and after 30 min, von Frey thresholds were measured. Animals were then either treated with vehicle or sanshool solution. Animals were tested again 60 min after sanshool/vehicle treatment. Solid bar represents the mean threshold. $n = 11$. $^*P < 0.05$ (Kruskal–Wallis test, Tukey's HSD *post hoc* test). *E*, response latency to radiant heat stimuli applied to the hindpaw in mice before and after MO treatment. MO was applied topically to the hindpaw, and after 30 min, animals were either treated with vehicle or sanshool solution. Animals were tested for response to radiant heat stimuli 60 min after sanshool/vehicle treatment. $n = 8$, 7 for vehicle and sanshool, respectively. $\#P < 0.05$ (two-way ANOVA, Tukey's HSD *post hoc* test). Error bars are S.E.M.

Table 1. Distribution of cutaneous sensory fibres that are activated or inhibited by sanshool

Fibre type	% activated (*n*)	% inhibited (*n*)
Aδ mechanoreceptor	2 (47)	88 (17)
Down hair	96 (23)	ND
Rapidly adapting Aβ	56 (27)	11 (9)
Slowly adapting Aβ	44 (34)	33 (15)
C	34 (68)	0 (17)

Fibres were stimulated with either a mechanical or an electrical stimulus. Data are from this study and Lennertz *et al.* (2010). ND, not determined.

(0.2% DMF), or sanshool (200 μM; Fig. 2*A*). Sanshool inhibited mechanically evoked AP firing in most AM fibres (90%) and a subset of slowly adapting Aβ fibres (38%) (Fig. 2*A–C*). In contrast, all mechanically sensitive C fibres continued to display mechanically evoked AP firing in the presence of sanshool (0%) (Fig. 2*A–C*). Fibre inhibition was concentration-dependent, with an IC_{50} of 70 ± 7 μM for AM fibres in response to 100 mN force (Fig. 2*D*). Sanshool inhibition was observed at a wide range of applied mechanical forces (Fig. 2*E*). A maximal inhibitory effect was observed after ~4 min of 200 μM sanshool application; in some AM fibres, such inhibition persisted for more than 30 min following the wash out of sanshool (data not shown). These data demonstrate that sanshool strongly inhibits mechanical responses in slowly-adapting, myelinated fibres, especially the AM fibres, which mediate sharp acute mechanical pain as well as the hypersensitivity to mechanical pain after neurogenic inflammation (Lin *et al.* 2000; Magerl *et al.* 2001). These findings are consistent with the use of toothache tree extracts to treat inflammatory hypersensitivity in areas densely innervated by myelinated mechanosensitive pain fibres (e.g. tooth pulp or joints) (Heppelmann *et al.* 1988; Paik *et al.* 2010).

Electrical excitability of sensory fibres and dissociated sensory neurons is suppressed by sanshool

Sanshool may attenuate mechanically evoked AP firing by either inhibiting mechanosensitive channels that trigger excitability, or by directly inhibiting voltage-gated channels. Thus, we questioned whether sanshool inhibits AP firing using an electrical stimulus, which would bypass mechanical transduction. We found that sanshool attenuated the electrically evoked AP firing in all AM fibres and in a subset of slowly adapting Aβ fibres, but in contrast had no effect on C fibres (Fig. 3*A* and *B*). The time course of recovery of electrical excitability correlated well with the recovery of mechanical excitability (data not shown). This experiment suggests that sanshool inhibits the initiation or propagation of APs in slowly adapting, myelinated fibres, independently of its effect on mechanical transduction.

Consistent with its effect on sensory fibres, sanshool also inhibited electrically evoked AP firing in a subset of cultured DRG neurons (Fig. 3*C* and *D*). Sanshool completely inhibited AP firing in 35% of neurons, and significantly reduced the AP amplitude in another 29% of sensory neurons following injection of suprathreshold current ($n = 31$; Fig. 3*D*). Another 36% were unaffected by sanshool. The sanshool-induced AP inhibition was concentration-dependent with an IC_{50} of 56 μM ($n = 4$, data not shown).

Sanshool-sensitive neurons had distinct physical and physiological characteristics compared to sanshool-resistant neurons. First, larger diameter neurons (>28 μm) were more likely to be inhibited by sanshool (nine of 16 large diameter *vs.* two of 15 small diameter; $P < 0.05$, Fisher's exact test). This result is consistent with the inhibition of myelinated fibres in our teased fibre recordings (Fig. 2). Small diameter neurons tend to express higher levels of Na_v channels that are resistant to the specific sodium channel blocker TTX, such as $Na_v1.8$, as compared to larger diameter neurons (Black *et al.* 1996; Fukuoka *et al.* 2008). Accordingly, the small diameter neurons that were insensitive to sanshool were also resistant to TTX (86%). Second, neurons inhibited by sanshool had a more hyperpolarized threshold for AP firing at baseline (Fig. 3*E*). Na_v channels expressed in sensory neurons are activated at different membrane potentials depending on the channel subtype (Rush *et al.* 2005). Therefore, sanshool-sensitive neurons may express Na_v channels that are activated at a more hyperpolarized membrane potential and are preferentially inhibited by sanshool.

Sanshool attenuates excitability by inhibiting voltage-gated sodium channels in dorsal root ganglion neurons

We next used whole-cell voltage clamp recording to examine the effects of sanshool on endogenous Na_v channels in sensory neurons. The application of sanshool caused a rapid and reversible reduction in voltage-gated sodium current amplitude (Fig. 4*A–D*). Classification of neurons based on their sensitivity to TTX showed that TTX sensitivity is weakly correlated with sanshool sensitivity (Fig. 4*E*).

Many Na_v channel inhibitors act by preferentially binding to the inactivated state of the channel, which promotes a hyperpolarizing shift in the steady-state inactivation curve (Hille, 1977; Bean *et al.* 1983). We thus measured voltage-dependent steady-state inactivation of Na_v channels in the absence and presence of sanshool (Fig. 4*F*). Sensory neurons express multiple

sodium channel subtypes that differ in sensitivity to voltage-dependent inactivation. As such, our data were best fit with either a single or a double Boltzmann function to determine a single or two midpoint(s) for inactivation (V_h), respectively (see Materials and methods for fit assumptions) (Rush *et al.* 2005; Kistner *et al.* 2010). Sanshool caused a significant hyperpolarizing shift in both V_{h1} and V_{h2} (Fig. 4*G*), suggesting that sanshool may promote steady-state inactivation at or near the resting potential.

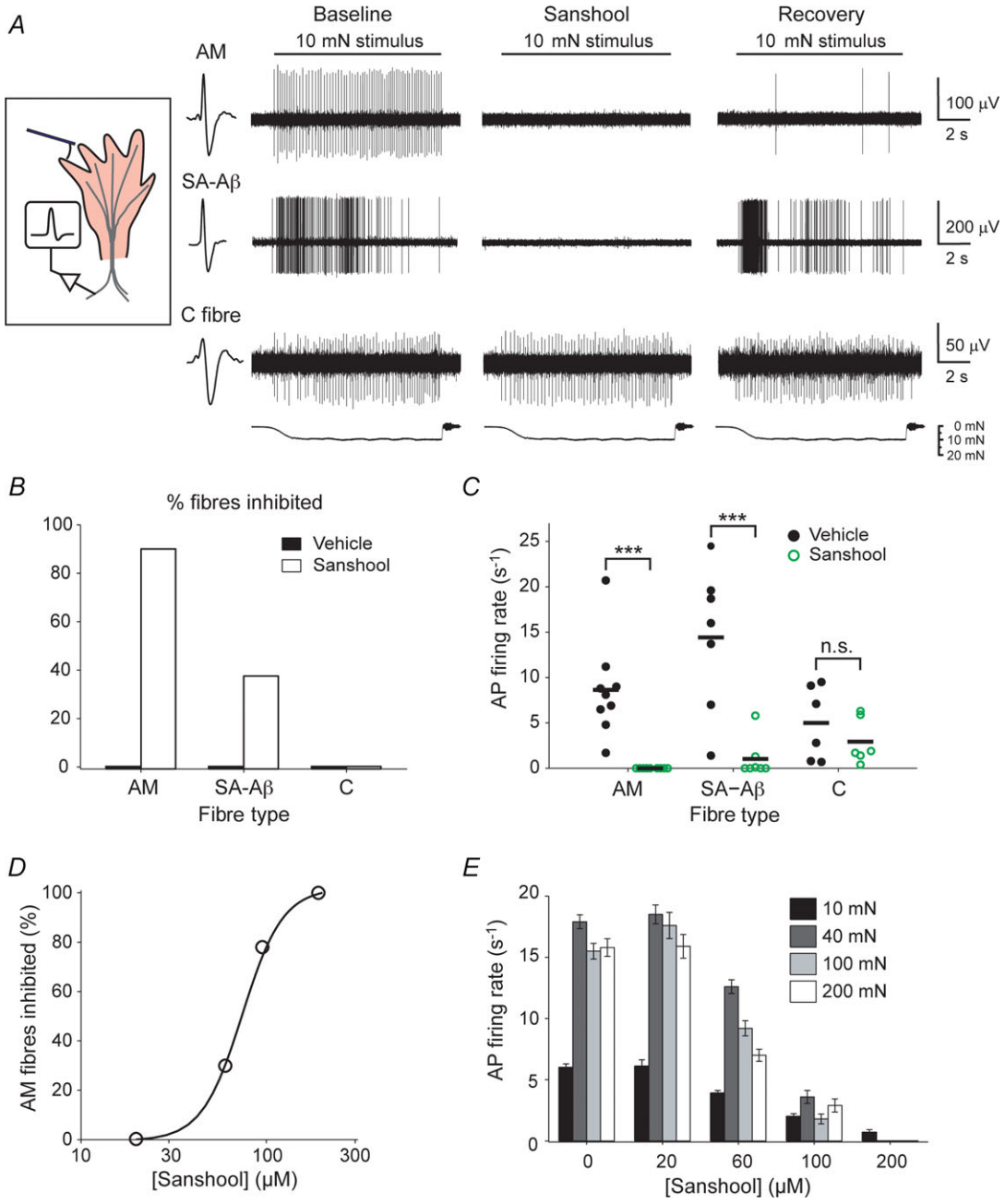

Figure 2. Sanshool suppresses mechanosensitivity of cutaneous somatosensory fibres
A, example recordings demonstrate the inhibition of mechanically evoked action potentials in SA-Aβ and AM fibres in the presence of sanshool. $P < 0.001$ (χ^2 test). $n = 8$–10. *C*, number of action potentials fired at baseline and after 3 min in sanshool for each fibre tested. Solid bar represents the mean. $^{***}P < 0.001$, (two-way ANOVA). $n = 8$–10. *D*, sanshool concentration–inhibition curve for AM fibres using a 100 mN force stimulus. Data were fitted by a non-linear four-parameter regression model. *E*, dose-dependent inhibition of AM fibres by sanshool in response to increasing mechanical force. $n = 9$–14. AM, Aδ mechanoreceptor; AP, action potential; C, C fibre; n.s., not significant; SA, slowly adapting.

Sodium channel subtypes are selectively sensitive to sanshool

If sanshool dampens sensory neuron excitability by inhibiting Na_v channels, sanshool sensitivity may correlate with the expression of sanshool-sensitive Na_v channel subtypes. Our initial characterization showed that sensory neurons expressing TTX-sensitive Na_v channels tend to be more strongly inhibited, while those expressing TTX-resistant Na_v channels are less suppressed by sanshool (Fig. 4*E*). However, TTX sensitivity of AP firing did not correlate strictly with sanshool sensitivity, as many TTX-sensitive large diameter neurons were still resistant to the inhibitory effect of sanshool. We thus sought to determine the specific Na_v channel subtypes expressed in neurons inhibited by sanshool.

Because molecular markers are not yet available to differentiate among somas of myelinated fibre subtypes in culture and soma size is a rough marker of functional subtypes, we used a 'next best' approach. We used calcium imaging to functionally classify neurons and then performed qPCR on subgroups of neurons to identify Na_v channel subtype expression. Neurons were classified into three groups based on soma size and calcium response to sanshool (Fig. 5*A*). Group I neurons are larger in diameter and activated by sanshool, as previously described (Lennertz *et al.* 2010). Group I neurons likely correspond to myelinated light touch receptors, including rapidly adapting Aβ, some slowly adapting Aβ and rapidly adapting Aδ fibres. Group II neurons are also large diameter but are not activated by sanshool,

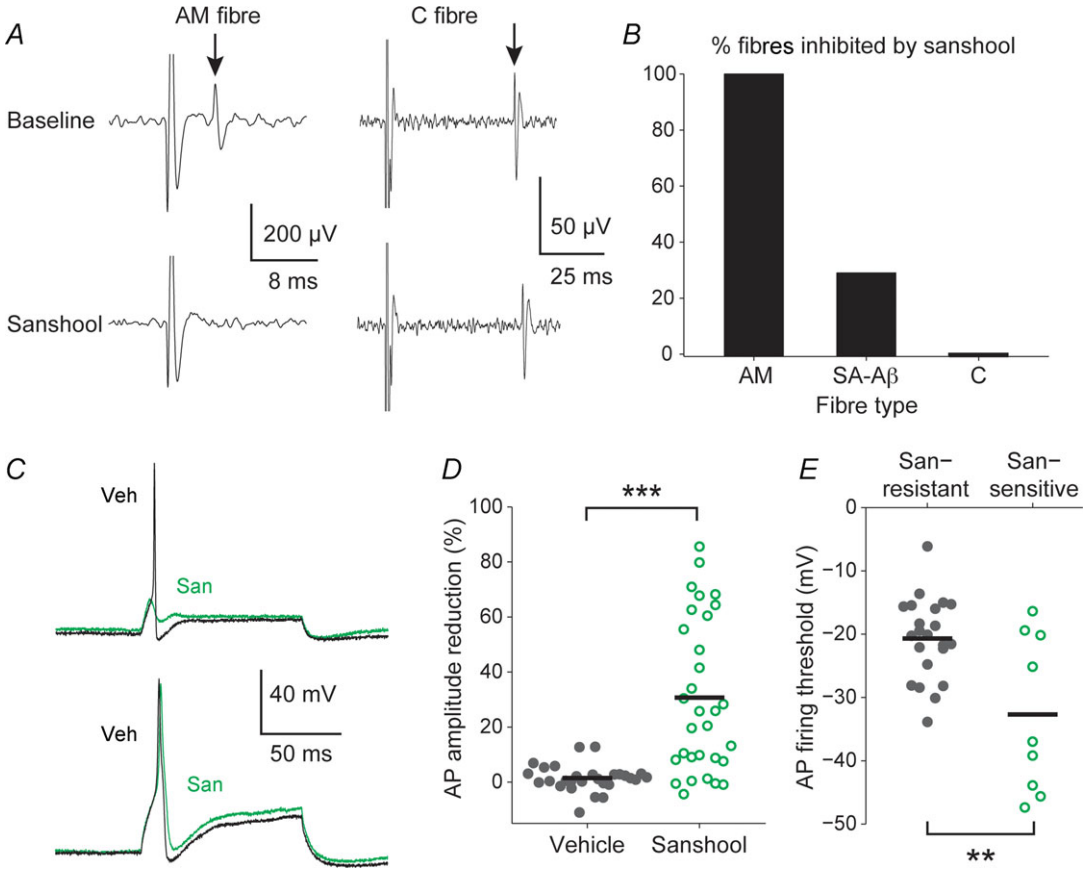

Figure 3. Sanshool suppresses electrical excitability in myelinated nociceptors
A, example recordings demonstrate the inhibition of electrically evoked action potentials in AM fibres but not in C fibres. *B*, percentage of nerve fibres that exhibit electrical inhibition in the presence of sanshool. $P < 0.001$ (χ^2 test). $n = 7$–9. Error bars are S.E.M. *C*, representative voltage traces of APs evoked by current injection in dorsal root ganglion neurons, in the presence of vehicle (black) or 200 μM sanshool (green). Some neurons failed to generate an AP (top) while others remained excitable (bottom) in the presence of sanshool. *D*, percentage inhibition of AP amplitude relative to baseline in the presence of vehicle (filled) or 200 μM sanshool (open) solution. Neurons that fired spontaneous APs in the presence of sanshool were not included in the analysis. $n = 31$. *E*, thresholds for AP firing in neurons resistant or sensitive to the inhibitory effect of sanshool. Neurons were classified using a 50% cut-off for sanshool-induced reduction in AP amplitude. AP firing threshold was defined as the potential at which the rate of change in membrane potential (dV/ds) was greater than 15 mV ms^{-1}. $n = 22$, 9 for sanshool-resistant and sanshool-sensitive neurons, respectively. $^{**}P < 0.01$, $^{***}P < 0.001$ (Student's *t* test). Error bars are S.E.M. AM, Aδ mechanoreceptor; AP, action potential; SA, slowly adapting; San, sanshool.

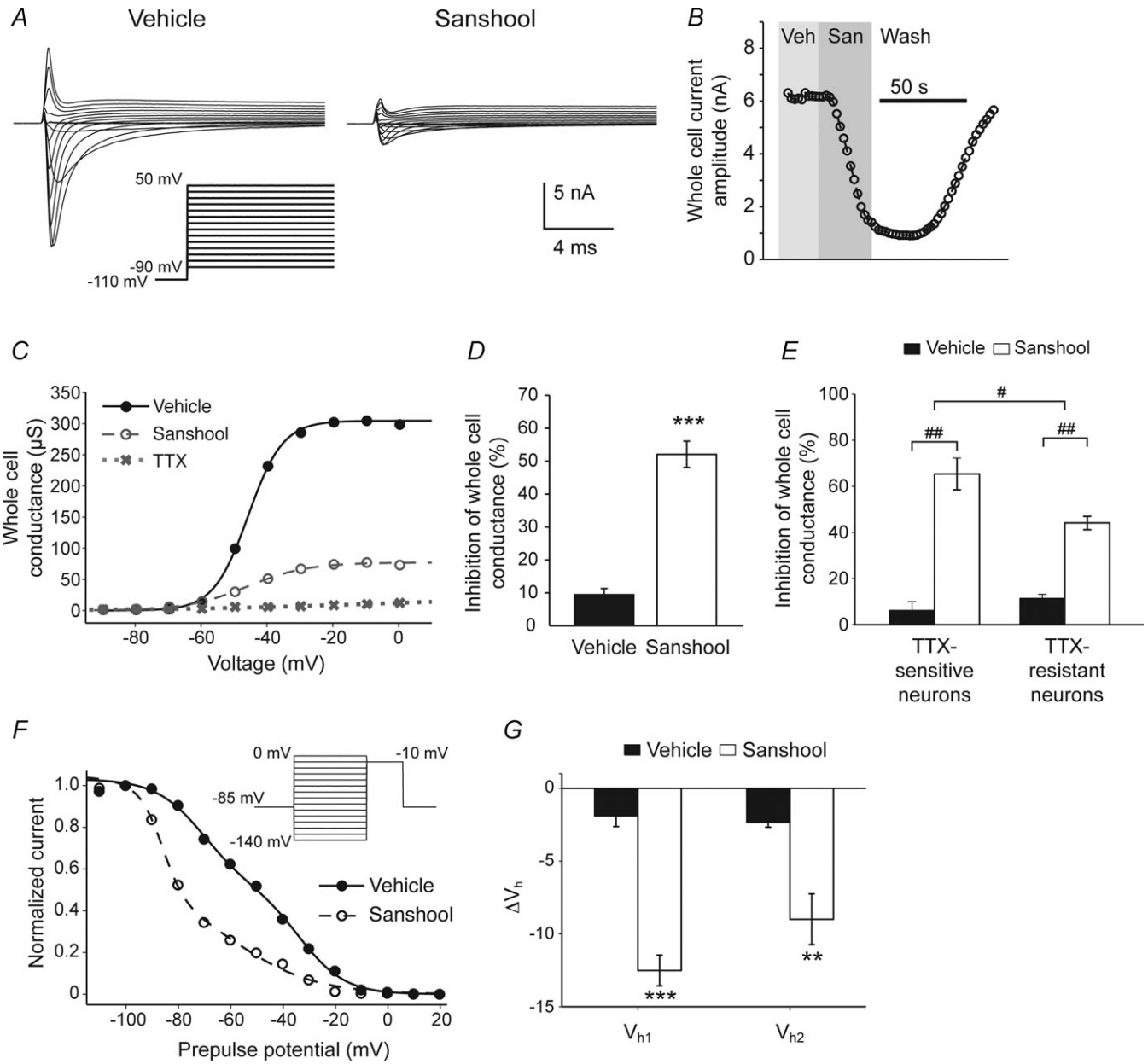

Figure 4. Endogenous voltage-gated sodium currents are inhibited by sanshool in cultured sensory neurons

A, representative voltage-gated sodium current traces from dissociated dorsal root ganglion (DRG) neurons, in the absence (left) and presence of sanshool (right, 200 μM). Inset shows the voltage protocol for the traces. *B*, representative time course of sanshool-induced voltage-gated sodium current inhibition. 30 ms step pulses from −110 mV to −20 mV were applied at 2 s intervals. Holding potential was −85 mV. Veh, vehicle; San, sanshool; Wash, washout. *C*, whole-cell voltage-gated sodium conductance of a representative DRG neuron shown in *A*. Data points were fit with a Boltzmann function. *D*, percentage inhibition of peak conductance relative to baseline in the presence of vehicle (filled) or 200 μM sanshool (open). 200 ms step pulses from −110 mV to −10 mV were applied. $n = 16$. *E*, percentage of suppression of total maximum conductance after stepping from −110 mV to −10 mV. Neurons were classified according to sensitivity to TTX. $n = 16$. #$P < 0.05$, ##$P < 0.01$, n.s. not significant (two-way ANOVA, Tukey's HSD *post hoc* test). *F*, representative voltage-dependent steady-state inactivation curve of a DRG neuron, in the absence and presence of sanshool (200 μM). Voltage protocol (inset) consisted of a 100 ms prepulse step to indicated potentials from a holding potential of −85 mV, followed by a 10 ms step to −10 mV. Data points were fit with a double Boltzmann function (see Methods). *G*, average shift in the midpoints of the steady-state inactivation curves derived from double Boltzmann fits. $n = 9$. **$P < 0.01$, ***$P < 0.001$ (Student's *t* test). TTX, tetrodotoxin.

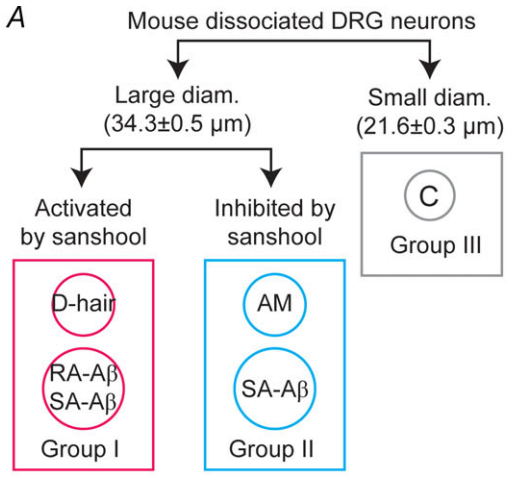

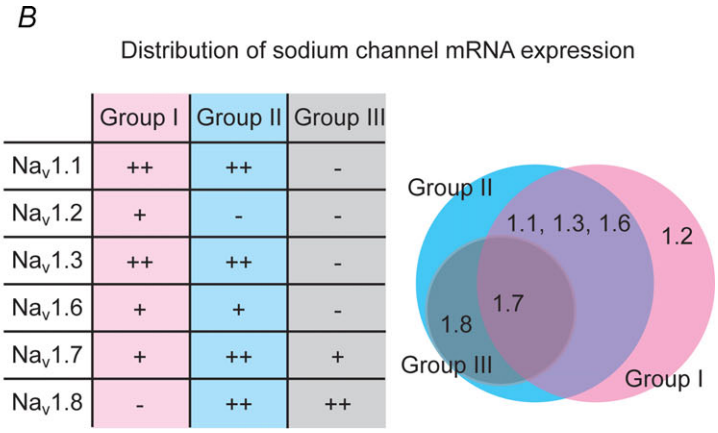

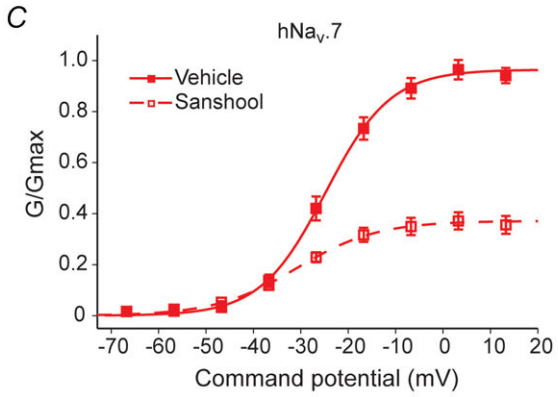

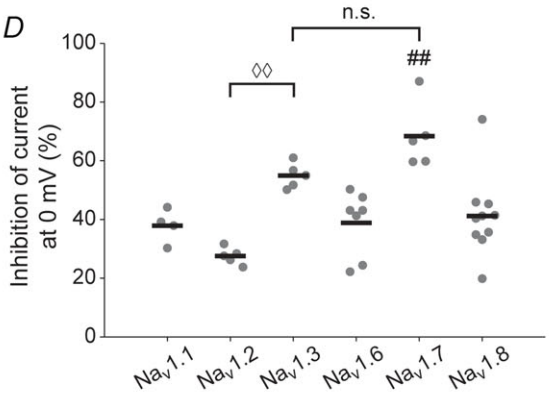

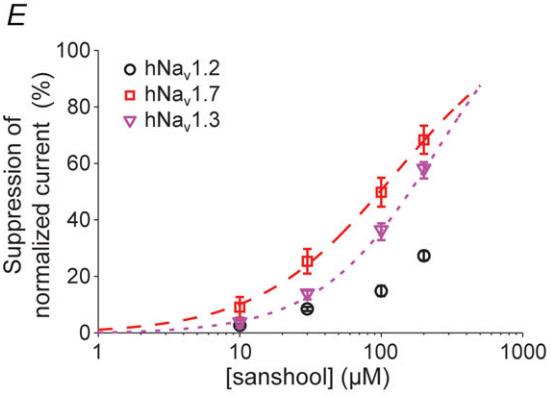

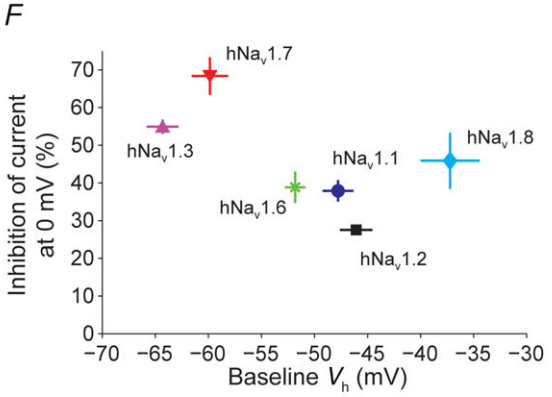

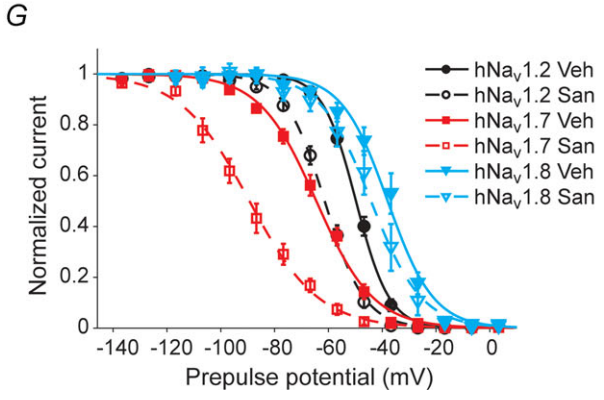

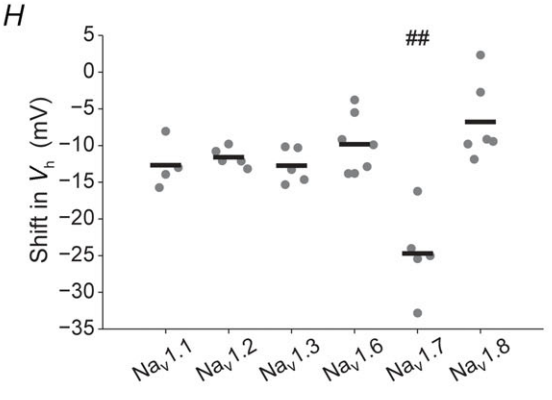

and represent neurons that are more likely to be silenced (AM and another subset of slowly adapting Aβ fibres) (Fig. 5*A*). Group III small diameter neurons are activated by capsaicin and thus include a population of C fibre nociceptors. Neurons from each group were pooled and Na_v channel mRNA expression levels were measured by qPCR.

The three groups of neurons displayed unique combinations of Na_v channel subtype expression (Fig. 5*B*, Supplemental Fig. 1). Group I neurons expressed all subtypes tested except for $Na_v1.8$. Similarly, group II neurons expressed most Na_v channel subtypes, including $Na_v1.8$, with the exception of $Na_v1.2$. Group III neurons only expressed $Na_v1.7$ and 1.8. These results are consistent with the previously described distribution of Na_v channel subtypes based on relative cell size (Black *et al.* 1996; Fukuoka *et al.* 2008; Ho & O'Leary, 2011). Notably, larger diameter neurons that express both $Na_v1.7$ and $Na_v1.8$ probably include Aδ nociceptors (Djouhri *et al.* 2003*a*,*b*). These data suggest that $Na_v1.2$ expression may underlie the resistance of larger diameter neurons to sanshool, and that $Na_v1.2$ may be more resistant to sanshool than other subtypes. To test this, we characterized the degree of current block at 0 mV and the shift in steady-state inactivation induced by sanshool in Na_v channel subtypes expressed heterologously.

All Na_v channels tested displayed voltage-gated currents that were reduced, to varying degrees, by sanshool (Fig. 5*C* and *D*). Notably, $Na_v1.3$ and 1.7 displayed significantly more block at 0 mV as compared to $Na_v1.1$, 1.2, 1.6 and 1.8, with $Na_v1.2$ displaying the least sensitivity (Fig. 5*D* and *E*). There are several classes of Na_v channel inhibitors that have different mechanisms of action. Local anaesthetics, such as lidocaine, act by binding to the open or inactivated state of Na_v channels (Hille, 1977; Ragsdale *et al.* 1994). Plotting the strength of sanshool-induced current inhibition against the mid-point for steady-state inactivation showed a clear correlation. The inhibition by sanshool tended to be stronger as the fraction of inactivated channels at resting potential increased (Fig. 5*F*). In DRG neurons, sanshool caused a hyperpolarizing shift in the steady-state inactivation curve of endogenous sodium channels (Fig. 4*F* and *G*). Interestingly, even though sanshool shifted the steady-state inactivation of all heterologously expressed Na_v channels, sanshool caused the biggest shift in $Na_v1.7$ (Fig. 5*G* and *H*). These results suggest that at resting potential, sanshool is likely to have the most profound inhibitory effect on the activity of $Na_v1.7$ channels. Overall, sanshool inhibits Na_v channel subtypes to varying degrees, and differences in the relative contribution of each channel subtype to excitability may dictate sanshool sensitivity among the different groups of neurons.

Discussion

Extracts from the toothache tree have been used for decades to treat inflammatory pain. Yet, the molecular mechanisms that mediate the analgesia remained unknown. Here we demonstrate that topical application of sanshool to the skin blocks mechanical but not heat hypersensitivity following inflammation. Our results suggest that sanshool induces analgesia by completely silencing

Figure 5. Sanshool preferentially targets $Na_v1.7$
A, schematic for classifying cultured sensory neurons based on calcium response properties to sanshool and capsaicin. Circle diameter represents relative cell body size, which in turn correlate with myelination. *B*, distribution of Na_v channel subtype expression in groups of dissociated somatosensory neurons classified as in *A*. (Left) Prevalence of Na_v channel subtype mRNA in different groups. Transcripts were detected in either >80% (++), between 80% and 50% (+), or <20% (–) of total samples tested. $n = 6$ samples. (Right) Summary of Na_v channel mRNA distribution in group I (red), group II (blue) and group III (grey) DRG neurons. *C*, conductance–voltage relationship of human $Na_v1.7$ expressed in Chinese hamster ovary cells, in the presence of vehicle or sanshool (200 μM). Data points were fit with a Boltzmann function. $n = 5$. *D*, percentage inhibition of current, relative to vehicle control, of the indicated human Na_v (hNa_v) channels by 200 μM sanshool. Cells were held at −80 mV and stepped to 0 mV following a 20 ms step to −100 mV. Solid bar represents the mean percentage of inhibition. $n = 4$–10. ##$P < 0.01$ compared to all others, except indicated otherwise, ◇◇$P < 0.01$, n.s. not significant (one-way ANOVA, Tukey's HSD *post hoc* test). *E*, dose–response of sanshool-induced current inhibition in $hNa_v1.2$, $hNa_v1.3$ and $hNa_v1.7$. Data points for $hNa_v1.7$ and $hNa_v1.3$ were fit with a four-parameter sigmoidal function, with a mean IC_{50} value of 124 and 249 μM, respectively. $n = 4$–5. $P < 0.001$ between $hNa_v1.2$, $hNa_v1.3$ and $hNa_v1.7$ (repeated measures ANOVA). *F*, relationship between mean percentage of sanshool-induced hNa_v inhibition and average midpoint for steady-state inactivation at baseline. Percentage current inhibition for each cell expressing hNa_v subtype was derived as in *D*. For steady-state inactivation, cells were held at −80 mV and stepped to the indicated prepulse potentials for 100 ms, followed by a 10 ms step to −5 mV. Data points were fit with a Boltzmann function to obtain the inactivation midpoint potential, V_h (see Methods). $n = 4$–7. *G*, steady-state inactivation curves of $hNa_v1.2$ (black), $hNa_v1.7$ (red) and $hNa_v1.8$ (blue) in the presence or absence of sanshool (200 μM). $n = 5$–6. San, sanshool; Veh,vehicle. *H*, shift in V_h for hNa_v channels in the presence of sanshool (200 μM) relative to vehicle control. Solid bar represents the mean shift. $n = 4$–7. ##$P < 0.01$ compared to all others (one-way ANOVA, Tukey's HSD *post hoc* test). Error bars are S.E.M. AM, Aδ mechanoreceptor; RA, rapidly adapting; SA, slowly adapting.

Aδ nociceptors through inhibition of Na_v channels and blockade of AP firing.

Selective silencing of myelinated nociceptors

Sanshool is commonly used to treat toothache and rheumatoid arthritis. Structural and staining studies have shown that many fibres innervating the tooth pulp and knee joints are lightly myelinated and have free nerve endings, indicative of Aδ nociceptors (Heppelmann *et al.* 1988; Paik *et al.* 2010). In addition, recordings from fibres innervating the knee joint confirm that many of these fibres display functional properties of Aδ fibres (Guilbaud *et al.* 1985). In models of inflammatory pain, both myelinated and unmyelinated nociceptors have lower response thresholds, increased spontaneous activity and higher stimulus-evoked AP firing rate (Guilbaud *et al.* 1985; Schaible & Schmidt, 1985). Aδ fibres in particular may be sensitized during neurogenic inflammation via the release of inflammatory mediators such as substance P that then sensitizes Aδ terminals (Herbert & Schmidt, 2001; Magerl *et al.* 2001). Thus sanshool may be a highly effective analgesic for inflammatory pain because of its preferential silencing of Aδ mechanonociceptors.

Differential inhibition of Na_v channel subtypes

The analgesic properties of sanshool resemble those of local anaesthetics (LAs) such as lidocaine, at both the physiological and molecular levels. LAs preferentially bind to the open and inactivated states of Na_v channels by binding to specific residues in the S6 segments within the ion-conduction pore (Hille, 1977; Ragsdale *et al.* 1994). Structure–function studies for an insecticidal alkylamide that is structurally related to sanshool showed that the residues in S6 required for LA activity are also important for inhibition by alkylamides (Du *et al.* 2011). The leftward shift in the steady-state inactivation curve induced by sanshool also suggests that sanshool may bind to the open and/or inactivated state of Na_v channels.

Like sanshool, LAs also display channel subtype specificity (Roy & Narahashi, 1992; Chevrier *et al.* 2004; Leffler *et al.* 2007; Kistner *et al.* 2010). For example, the efficacy of block by lidocaine is dependent on the fraction of inactivated channels present at a given membrane potential, and this fraction varies between channel subtypes (Wright *et al.* 1997; Herzog *et al.* 2003; Rush *et al.* 2005; Leffler *et al.* 2007; Kistner *et al.* 2010). The different subtypes of Na_v channels expressed in DRG neurons also displayed varying degrees of sanshool-induced tonic inhibition at resting potentials (Fig. 5). $Na_v1.7$ and 1.3 display the most hyperpolarized steady-state inactivation, indicating that more channels are inactivated at rest compared to other DRG neuron sodium channels, such as $Na_v1.2$. This in turn would allow sanshool to inhibit $Na_v1.7$ and 1.3 more potently than $Na_v1.2$. Although both $Na_v1.7$ and 1.3 voltage-gated currents were inhibited strongly by sanshool, $Na_v1.7$ was unique in that its steady-state inactivation curve was shifted significantly more compared to other subtypes (Fig. 5). Thus the potent, dual action of sanshool on the current magnitude and steady-state inactivation properties of $Na_v1.7$ may make this channel subtype particularly susceptible to sanshool.

Na_v channel subtypes in sensory fibre function

Our Na_v channel subtype expression and sanshool-sensitivity analyses (Fig. 5) suggest a model in which somatosensory neurons can be classified functionally based on their dependence on distinct but overlapping sets of Na_v channel subtypes for maintaining excitability. Aδ nociceptors and slowly adapting Aβ fibres (represented by group II neurons) may be more likely to be inhibited by sanshool because they rely on $Na_v1.7$ and/or $Na_v1.3$. In contrast, rapidly adapting Aβ fibres (represented by group I neurons) are resistant to sanshool possibly because they rely less on $Na_v1.7$ and/or $Na_v1.3$ for excitability. C fibres (represented by group III neurons) are also resistant to sanshool because they rely on $Na_v1.8$, which is more resistant to sanshool as compared to $Na_v1.7$. These results support a model in which different Na_v channels play specific roles in somatosenosory neuron function.

Unfortunately, we were unable to probe the sanshool sensitivity of Nav1.9 as there is no readily available and reliable source of Nav1.9 expressing cell lines. However, Nav1.9 is unlikely to play a key role in sanshool-evoked neuronal silencing because expression is limited to small diameter neurons and is unlikely to contribute to excitability of the sanshool-sensitive neurons (Fukuoka *et al.* 2008; Ho & O'Leary, 2011). In addition, Nav1.9 does not contribute to the rising phase of the AP (Herzog *et al.* 2001; Waxman & Estacion, 2008), thus it is unclear how sanshool sensitivity would affect AP firing.

The role of $Na_v1.3$ in somatosensory neurons remains enigmatic. Expression of $Na_v1.3$ is robust embryonically and after axotomy or nerve injury, but is otherwise weak (Waxman *et al.* 1994; Black *et al.* 1999; Kim *et al.* 2001). In addition, $Na_v1.3$ expression is robust in dissociated DRG cultures whereas very little is detected *in situ* in tissue slices (Black *et al.* 1996). Likewise, our results showed robust expression of $Na_v1.3$ in dissociated group I and II neurons. Thus, the relative contribution of $Na_v1.3$ to sanshool sensitivity *in vivo* is unclear.

Previous studies of Na_v channel subtype expression in DRG neurons suggest that $Na_v1.7$ is expressed in a large population of neurons (Black *et al.* 1996; Fukuoka *et al.* 2008; Ho & O'Leary, 2011). Aδ nociceptors in particular express relatively high levels of $Na_v1.7$ as well as $Na_v1.8$

(Djouhri *et al.* 2003*a*,*b*). In addition, $Na_v1.7$ expression is upregulated during inflammation of the tooth pulp and joints (Luo *et al.* 2008; Strickland *et al.* 2008). However, the functional contribution of each Na_v subtype in Aδ nociceptors is not known. Our results implicate $Na_v1.7$ as a critical mediator of Aδ nociceptor excitability, perhaps due to its proposed role in impulse initiation (Cummins *et al.* 1998). Consistent with this model, $Na_v1.7$ expression has been observed in nerve endings of cutaneous myelinated nociceptors (Black *et al.* 2012). Future fibre recordings using $Na_v1.7$ and $Na_v1.8$ knockout mice, or $Na_v1.7$-specific inhibitors (not commercially available), are needed to test this hypothesis.

$Na_v1.7$ is also expressed in a subset of Aβ fibres that respond to gentle mechanical stimulation (Djouhri *et al.* 2003*b*). Our results suggest that $Na_v1.7$ may also contribute to AP firing in a subset of slowly adapting Aβ fibres. The functional consequence of inhibiting $Na_v1.7$ in these fibres is unclear. However, the reduced behavioural mechanosensitivity induced by sanshool in naïve animals may partly be due to sanshool's inhibitory effect on these tactile fibres.

Many unmyelinated nociceptors also express $Na_v1.7$ and $Na_v1.8$ (Black *et al.* 1996; Djouhri *et al.* 2003*a*,*b*; Fukuoka *et al.* 2008; Ho & O'Leary, 2011; Shields *et al.* 2012). However, C fibres remained largely resistant to the inhibitory effect of sanshool. While our PCR results suggest that $Na_v1.8$ mRNA is expressed at similar levels between group II and group III neurons (Supplementary Fig. 1), there may be differential expression of $Na_v1.8$ protein. In addition, electrophysiologically, unmyelinated nociceptors appear to rely more on $Na_v1.8$ for AP generation (Blair & Bean, 2002). Indeed, the relative resistance of C fibres to lidocaine is thought to be due to high expression of $Na_v1.8$ in these fibres (Kistner *et al.* 2010). Thus, sanshool resistance of C fibres may also be due to their reliance on $Na_v1.8$, which is relatively insensitive to sanshool, for initiation of APs.

Acute, peripheral inhibition of mechanical pain by sanshool

We have previously shown that sanshool activates a subset of primary afferents, including Aβ fibres to induce tingling paraesthesia (Table 1) (Lennertz *et al.* 2010). Thus, it is possible sanshool-evoked analgesia may be indirect, as Aβ fibre activity can modulate nociceptor activity through central inhibition (Melzack & Wall, 1965; Woolf *et al.* 1980). However, central inhibition would be expected to alter both mechanical and thermal responsiveness (Chung *et al.* 1984; Paik *et al.* 1988) and cannot explain the activity of sanshool in the skin–nerve or *in vivo* experiments. Thus our data support a model whereby sanshool directly inhibits peripheral nociceptor terminals to mediate analgesia.

Studies on Na_v channel knockout mice have shown significant roles for $Na_v1.7$ in somatosensory behaviour. $Na_v1.7$ is required for normal responses to radiant heat and noxious mechanical stimuli, but this channel is not required for responses to a noxious hot plate (Minett *et al.* 2012). As such, it has been proposed that neurons that predominantly depend on $Na_v1.7$ are involved in acute thermal pain responses, while neurons that express both $Na_v1.7$ and $Na_v1.8$ mediate mechanical and inflammatory pain (Nassar *et al.* 2004; Minett *et al.* 2012). Humans with loss of function mutations in $Na_v1.7$ do not experience pain in response to noxious mechanical or thermal stimuli (Cox *et al.* 2006). The lack of an effect of sanshool on thermal sensitivity was surprising given these studies. However, differences between acute inhibition of function and chronic genetic loss of $Na_v1.7$ through development may account for such differences. Additionally, inhibition of other channel subtypes by sanshool may contribute to the specificity of sanshool action. One such possibility might suggest that the dual suppression of $Na_v1.7$ and $Na_v1.3$ by sanshool results in selective silencing of Aδ mechanoreceptors and subsequent inhibition of mechanical pain. Regardless, our data offer insights into the mechanism by which modality-specific analgesia is induced by sanshool. In addition, the development of synthetic sanshool derivatives (Wu *et al.* 2012) may be useful for treating painful inflammatory conditions that involve sensitization of myelinated mechanosensitive nociceptors.

References

Bautista DM, Sigal YM, Milstein AD, Garrison JL, Zorn JA, Tsuruda PR, Nicoll RA & Julius D (2008). Pungent agents from Szechuan peppers excite sensory neurons by inhibiting two-pore potassium channels. *Nat Neurosci* **11**, 772–779.

Bean BP, Cohen CJ & Tsien RW (1983). Lidocaine block of cardiac sodium channels. *J Gen Physiol* **81**, 613–642.

Black JA, Dib-Hajj S, McNabola K, Jeste S, Rizzo MA, Kocsis JD & Waxman SG (1996). Spinal sensory neurons express multiple sodium channel alpha-subunit mRNAs. *Brain Res Mol Brain Res* **43**, 117–131.

Black JA, Cummins TR, Plumpton C, Chen YH, Hormuzdiar W, Clare JJ & Waxman SG (1999). Upregulation of a silent sodium channel after peripheral, but not central, nerve injury in DRG neurons. *J Neurophysiol* **82**, 2776–2785.

Black JA, Frézel N, Dib-Hajj SD & Waxman SG (2012). Expression of Nav1.7 in DRG neurons extends from peripheral terminals in the skin to central preterminal branches and terminals in the dorsal horn. *Mol Pain* **8**, 82.

Blair NT & Bean BP (2002). Roles of tetrodotoxin (TTX)-sensitive Na^+ current, TTX-resistant Na^+ current, and Ca^{2+} current in the action potentials of nociceptive sensory neurons. *J Neurosci* **22**, 10277–10290.

Brown AG & Iggo A (1967). A quantitative study of cutaneous receptors and afferent fibres in the cat and rabbit. *J Physiol* **193**, 707–733.

Bryant BP & Mezine I (1999). Alkylamides that produce tingling paresthesia activate tactile and thermal trigeminal neurons. *Brain Res* **842**, 452–460.

Cao YQ, Mantyh PW, Carlson EJ, Gillespie AM, Epstein CJ & Basbaum AI (1998). Primary afferent tachykinins are required to experience moderate to intense pain. *Nature* **392**, 390–394.

Chaplan SR, Bach FW, Pogrel JW, Chung JM & Yaksh TL (1994). Quantitative assessment of tactile allodynia in the rat paw. *J Neurosci Methods* **53**, 55–63.

Chevrier P, Vijayaragavan K & Chahine M (2004). Differential modulation of Nav1.7 and Nav1.8 peripheral nerve sodium channels by the local anesthetic lidocaine. *Br J Pharmacol* **142**, 576–584.

Chung JM, Lee KH, Hori Y, Endo K & Willis WD (1984). Factors influencing peripheral nerve stimulation produced inhibition of primate spinothalamic tract cells. *Pain* **19**, 277–293.

Cox JJ, Reimann F, Nicholas AK, Thornton G, Roberts E, Springell K, Karbani G, Jafri H, Mannan J, Raashid Y, Al-Gazali L, Hamamy H, Valente EM, Gorman S, Williams R, McHale DP, Wood JN, Gribble FM & Woods CG (2006). An SCN9A channelopathy causes congenital inability to experience pain. *Nature* **444**, 894–898.

Cummins TR, Howe JR & Waxman SG (1998). Slow closed-state inactivation: a novel mechanism underlying ramp currents in cells expressing the hNE/PN1 sodium channel. *J Neurosci* **18**, 9607–9619.

Djouhri L, Fang X, Okuse K, Wood JN, Berry CM & Lawson SN (2003*a*). The TTX-resistant sodium channel Nav1.8 (SNS/PN3): expression and correlation with membrane properties in rat nociceptive primary afferent neurons. *J Physiol* **550**, 739–752.

Djouhri L, Newton R, Levinson SR, Berry CM, Carruthers B & Lawson SN (2003*b*). Sensory and electrophysiological properties of guinea-pig sensory neurones expressing Nav 1.7 (PN1) Na^+ channel subunit protein. *J Physiol* **546**, 565–576.

Du Y, Garden D, Khambay B, Zhorov BS & Dong K (2011). Batrachotoxin, pyrethroids, and BTG 502 share overlapping binding sites on insect sodium channels. *Mol Pharmacol* **80**, 426–433.

Eijkelkamp N, Linley JE, Baker MD, Minett MS, Cregg R, Werdehausen R, Rugiero F & Wood JN (2012). Neurological perspectives on voltage-gated sodium channels. *Brain* **135**, 2585–2612.

Foster S & Duke JA (1999). Zanthoxylum. In *A Field Guide to Medicinal Plants and Herbs: Of Eastern and Central North America*, 2nd edn., ed. Peterson RT, pp. 268–269. Houghton Mifflin Harcourt, Boston.

Fukuoka T, Kobayashi K, Yamanaka H, Obata K, Dai Y & Noguchi K (2008). Comparative study of the distribution of the alpha-subunits of voltage-gated sodium channels in normal and axotomized rat dorsal root ganglion neurons. *J Comp Neurol* **510**, 188–206.

Guilbaud G, Iggo A & Tegnér R (1985). Sensory receptors in ankle joint capsules of normal and arthritic rats. *Exp Brain Res* **58**, 29–40.

Hargreaves K, Dubner R, Brown F, Flores C & Joris J (1988). A new and sensitive method for measuring thermal nociception. *Pain* **32**, 77–88.

Harper BYAA & Lawson SN (1985). Conduction velocity is related to morphological cell type in rat dorsal root ganglion neurones. *J Physiol* **359**, 31–46.

Heppelmann B, Heuss C & Schmidt RF (1988). Fiber size distribution of myelinated and unmyelinated axons in the medial and posterior articular nerves of the cat's knee joint. *Somatosens Mot Res* **5**, 273–281.

Herbert MK & Schmidt RF (2001). Sensitisation of group III articular afferents to mechanical stimuli by substance P. *Inflamm Res* **50**, 275–282.

Herzog RI, Cummins TR & Waxman SG (2001). Persistent TTX-resistant Na^+ current affects resting potential and response to depolarization in simulated spinal sensory neurons. *J Neurophysiol* **86**, 1351–1364.

Herzog RI, Cummins TR, Ghassemi F, Dib-Hajj SD & Waxman SG (2003). Distinct repriming and closed-state inactivation kinetics of Nav1.6 and Nav1.7 sodium channels in mouse spinal sensory neurons. *J Physiol* **551**, 741–750.

Hille B (1977). Local anesthetics: hydrophilic and hydrophobic pathways for the drug-receptor reaction. *J Gen Physiol* **69**, 497–515.

Ho C & O'Leary ME (2011). Single-cell analysis of sodium channel expression in dorsal root ganglion neurons. *Mol Cell Neurosci* **46**, 159–166.

Iggo A (1960). Cutaneous mechanoreceptors with afferent C fibres. *J Physiol* **152**, 337–353.

Kim CH, Oh Y, Chung JM & Chung K (2001). The changes in expression of three subtypes of TTX sensitive sodium channels in sensory neurons after spinal nerve ligation. **95**, 153–161.

Kistner K, Zimmermann K, Ehnert C, Reeh PW & Leffler A (2010). The tetrodotoxin-resistant Na^+ channel Nav1.8 reduces the potency of local anesthetics in blocking C-fiber nociceptors. *Eur J Physiol* **459**, 751–763.

Koltzenburg M, Stucky CL & Lewin GR (1997). Receptive properties of mouse sensory neurons innervating hairy skin receptive properties of mouse sensory neurons innervating hairy skin. *J Neurophysiol* **78**, 1841–1850.

Kwan KY, Glazer JM, Corey DP, Rice FL & Stucky CL (2009). TRPA1 modulates mechanotransduction in cutaneous sensory neurons. *J Neurosci* **29**, 4808–4819.

Leffler A, Reiprich A, Mohapatra DP & Nau C (2007). Use-dependent block by lidocaine but not amitriptyline is more pronounced in tetrodotoxin (TTX)-resistant Nav1.8 than in TTX-sensitive Na^+ channels. *J Pharmacol Exp Ther* **320**, 354–364.

Lennertz RC, Tsunozaki M, Bautista DM & Stucky CL (2010). Physiological basis of tingling paresthesia evoked by hydroxy-alpha-sanshool. *J Neurosci* **30**, 4353–4361.

Lin Q, Zou X & Willis WD (2000). Aδ and C primary afferents convey dorsal root reflexes after intradermal injection of capsaicin in rats. *J Neurophysiol* **84**, 2695–2698.

Lopez-Santiago LF, Pertin M, Morisod X, Chen C, Hong S, Wiley J, Decosterd I & Isom LL (2006). Sodium channel beta2 subunits regulate tetrodotoxin-sensitive sodium channels in small dorsal root ganglion neurons and modulate the response to pain. *J Neurosci* **26**, 7984–7994.

Lumpkin EA, Marshall KL & Nelson AM (2010). The cell biology of touch. *J Cell Biol* **191**, 237–248.

Luo S, Perry GM, Levinson SR & Henry M a (2008). Nav1.7 expression is increased in painful human dental pulp. *Mol Pain* **4**, 16.

Magerl W, Fuchs PN, Meyer RA & Treede RD (2001). Roles of capsaicin-insensitive nociceptors in cutaneous pain and secondary hyperalgesia. *Brain* **124**, 1754–1764.

Malin SA, Davis BM & Molliver DC (2007). Production of dissociated sensory neuron cultures and considerations for their use in studying neuronal function and plasticity. *Nat Protoc* **2**, 152–160.

McGlone F & Reilly D (2010). The cutaneous sensory system. *Neurosci Biobehav Rev* **34**, 148–159.

Melzack R & Wall PD (1965). Pain mechanisms: a new theory. *Science* **150**, 971–979.

Minett MS, Nassar M a, Clark AK, Passmore G, Dickenson AH, Wang F, Malcangio M & Wood JN (2012). Distinct Nav1.7-dependent pain sensations require different sets of sensory and sympathetic neurons. *Nat Commun* **3**, 791.

Nassar MA, Stirling LC, Forlani G, Baker MD, Matthews E a, Dickenson AH & Wood JN (2004). Nociceptor-specific gene deletion reveals a major role for Nav1.7 (PN1) in acute and inflammatory pain. *Proc Natl Acad Sci U S A* **101**, 12706–12711.

Paik KS, Nam SC & Chung JM (1988). Differential inhibition produced by peripheral conditioning stimulation on noxious mechanical and thermal responses of different classes of spinal neurons in the cat. *Exp Neurol* **99**, 498–511.

Paik SK, Lee DS, Kim JY, Bae JY, Cho YS, Ahn DK, Yoshida A & Bae YC (2010). Quantitative ultrastructural analysis of the neurofilament 200-positive axons in the rat dental pulp. *J Endod* **36**, 1638–1642.

Pereira SS, Lopes LS, Marques RB, Figueiredo K a, Costa D a, Chaves MH & Almeida FRC (2010). Antinociceptive effect of Zanthoxylum rhoifolium Lam. (Rutaceae) in models of acute pain in rodents. *J Ethnopharmacol* **129**, 227–231.

Ragsdale DS, McPhee JC, Scheuer T & Catterall W a (1994). Molecular determinants of state-dependent block of Na^+ channels by local anesthetics. *Science* **265**, 1724–1728.

Reeh PW (1986). Sensory receptors in mammalian skin in an in vitro preparation. *Neurosci Lett* **66**, 141–146.

Roy ML & Narahashi T (1992). Differential properties ganglion neurons of tetrodotoxin-sensitive and sodium channels in rat dorsal root. *J Neurosci* **7212**, 2104–2111.

Rush AM, Dib-hajj SD & Waxman SG (2005). Electrophysiological properties of two axonal sodium channels, Nav1.2 and Nav1.6, expressed in mouse spinal sensory neurones. *J Physiol* **3**, 803–815.

Rush AM, Cummins TR & Waxman SG (2007). Multiple sodium channels and their roles in electrogenesis within dorsal root ganglion neurons. *J Physiol* **579**, 1–14.

Schaible HG & Schmidt RF (1985). Effects of an experimental arthritis on the sensory properties of fine articular afferent units. *J Neurophysiol* **54**, 1109–1122.

Shields SD, Ahn H, Yang Y, Han C, Seal RP, Wood JN, Waxman SG & Dib-hajj SD (2012). Nav1.8 expression is not restricted to nociceptors in mouse peripheral nervous system. *Pain* **153**, 2017–2030.

Smith ESJ & Lewin GR (2009). Nociceptors: a phylogenetic view. *J Comp Physiol A Neuroethol Sens Neural Behav Physiol* **195**, 1089–1106.

Strickland IT, Martindale JC, Woodhams PL, Reeve AJ, Chessell IP & McQueen DS (2008). Changes in the expression of NaV1.7, NaV1.8 and NaV1.9 in a distinct population of dorsal root ganglia innervating the rat knee joint in a model of chronic inflammatory joint pain. *Eur J Pain* **12**, 564–572.

Sugai E, Morimitsu Y, Iwasaki Y, Morita A, Watanabe T & Kubota K (2005*a*). Pungent qualities of sanshool-related compounds evaluated by a sensory test and activation of rat TRPV1. *Biosci Biotechnol Biochem* **69**, 1951–1957.

Sugai E, Morimitsu Y & Kubota K (2005*b*). Quantitative analysis of sanshool compounds in Japanese pepper (Xanthoxylum piperitum DC.) and their pungent characteristics. *Biosci Biotechnol Biochem* **69**, 1958–1962.

Waxman SG & Estacion M (2008). Nav1.9, G-proteins, and nociceptors. *J Physiol* **586**, 917–918.

Waxman SG, Kocsis JD & Black JA (1994). Type III sodium channel mRNA is expressed in embryonic but not adult spinal sensory neurons, and is reexpressed following axotomy. *J Neurophysiol* **72**, 466–470.

Woolf CJ, Mitchell D & Barrett GD (1980). Antinociceptive effect of peripheral segmental electrical stimulation in the rat. *Pain* **8**, 237–252.

Wright SN, Wang SY, Kallen RG & Wang GK (1997). Differences in steady-state inactivation between Na channel isoforms affect local anesthetic binding affinity. *Biophys J* **73**, 779–788.

Wu B, Li K & Toy P (2012). Synthesis of hydroxy-α-sanshool. *Synlett* **23**, 2564–2566.

Zimmermann K, Leffler A, Babes A, Cendan CM, Carr RW, Kobayashi J, Nau C, Wood JN & Reeh PW (2007). Sensory neuron sodium channel Nav1.8 is essential for pain at low temperatures. *Nature* **447**, 855–858.

Additional information

Competing interests

None.

Author contributions

M.T. was responsible for the conception and design of experiments; collection, analysis and interpretation of data; drafting the article. R.C.L. was involved in the conception and design of experiments; collection, analysis and interpretation of data; drafting the article. D.V. dealt with the collection, analysis and interpretation of data. S.K. was involved in the collection, analysis and interpretation of data. C.L.S. contributed towards the conception and design of experiments and drafting of the article. D.M.B. was involved in the conception and design of experiments and drafting of the article. All authors approved the final version of the manuscript.

Behavioural assays, cellular electrophysiology and molecular biology were performed at UC Berkeley. *Ex-vivo* skin–nerve experiments and cellular electrophysiology were carried out at Medical College of Wisconsin.

Funding

This work was supported by the National Institutes of Health grants NS40538 and NS070711 to C.L.S. and AR059385 and DOD007123A to D.M.B.

Acknowledgements

We would like to thank Ted Cummins for generously providing the $Na_v1.7$-expressing human embryonic kidney cell line and members of our labs for useful discussions.